Lithium ion batteries

Equation of lithium oxidation, typically the anode
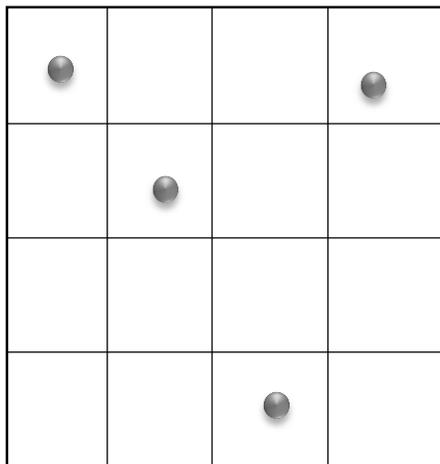
$$Li \rightleftharpoons Li + e^-, \qquad n = 1$$
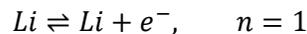
Where n is the number of electrons exchanged in the reaction.

Equation of intercalation into a host material M, typically the cathode

$$Li^+ + e^- + s \cdot M \rightarrow LiM_s$$
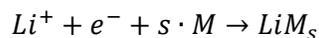
Lattice gas model of lithium intercalation in host layered oxide

Gibbs free energy of electrochemical reactions

$$G = H - TS + \sum_i z_i e \phi$$

with z_i, e, and ϕ respectively the ion valence, the electron charge, and the mean electrostatic potential applied at the electrode.

Under charge conservation for a mono-ionic system such as Li-Ion batteries.

$$N = \sum_i z_i$$

Phase entropy as a function of lithium filling in the layered oxide

$$S = K_B \ln(\Omega), \quad Boltzman\ configuration\ entropy$$

With Ω the configuration multiplicity (number of ways the inserted lithium cations could be arranged in the host lattice).

Under the reasonable assumption of indistinguishable lithium cations, the configuration multiplicity of N lithium cations into the host material with Ns *effective* total number of sites follows the combinatorial equation below:

$$\Omega = \binom{N_s}{N} = \frac{N_s!}{N!\,(N_s - N)!}, \quad \textit{configuration multiplicity of N particles on } N_s \textit{ sites}$$

Note: Ns is the *effective* number of lattice sites accounting for exclusions rules.

<u>Stirling approximation</u>

Simplification of the configuration necessitates the Stirling approximation of the logarithm of a factorial:

$$\ln(A!) = A\ln(A) - A, \quad \textit{Stirling approximation}$$

Readers are directed to the following website for proof to the above approximation: http://mathworld.wolfram.com/StirlingsApproximation.html

Hence,

$$
\begin{aligned}
S &= K_B\{\ln(N_s!) - \ln(N!) - \ln[(N_s - N)\,!]\} \\
&= K_B\{N_s \ln N_s - N_s - N\ln N + N - (N_s - N)\ln(N_s - N) + (N_s - N)\} \\
&= K_B\{N_s \ln N_s - N\ln N - (N_s - N)\ln(N_s - N)\} \\
&= K_B\{N_s[\ln N_s - \ln(N_s - N)] + N[-\ln N + \ln(N_s - N)]\} \\
&= K_B\left\{-N_s \cdot \ln\frac{N_s - N}{N_s} + N \cdot \ln\frac{N_s - N}{N}\right\}
\end{aligned}
$$

Let x be the fraction of sites occupied by cations such that

$$x = \frac{N}{N_s}$$

Then,

$$S = K_B N_s\left\{x \cdot \ln\left(\frac{1}{x} - 1\right) - \ln(1 - x)\right\}$$

$$S = -K_B N_s\{x \cdot \ln(x) + (1 - x)\cdot \ln(1 - x)\}$$

And

$$G = H - TS + Ne\phi, \quad \textit{Gibbs free energy of electrochemical reaction}$$

$$g = \frac{G}{N_s} = \frac{H}{N_s} - T\frac{S}{N_s} + \frac{N}{N_s}e\phi = h - Ts + xe\phi, \quad \textit{free energy per site}$$

$$\mu = \frac{dg}{dx} = \frac{dh}{dx} - T\frac{ds}{dx} + e\phi$$

$$\mu = \frac{dh}{dx} + K_B T \cdot \ln\left(\frac{x}{1 - x}\right) + e\phi, \quad \textit{electrochemical potential for single valent cation}$$

For a multivalent cation with valence number "z", it is straightforward to show that the electron energy term is scaled by "z" such that:

$$\mu = \frac{dh}{dx} + K_B T \cdot \ln\left(\frac{x}{1 - x}\right) + ze\phi, \quad \textit{electrochemical potential for multivalent cation}$$

It follows then that

Reactants activity:

Generally, the chemical potential of a species is related to the entropic term of the chemical potential.

$$\mu_{entropic}^i = K_B T ln(a_i)$$

Dilute solution approximation

The assumption of dilute solution states that the filling fraction is much less than 1. This results in the following simplified expression for the entropic term of the chemical potential.

$$\mu_{entropic} = K_B T ln(x)$$

And thus,

$$a_i = x = \frac{concentration\ c}{reference\ concentration\ c_{ref}}$$

Note: c_{ref} is usually defined at standard conditions (one molar ion contraction or 1 atm gas pressure)

Under concentrated (but still non-interacting, ideal) solution conditions, a non-neglible excess chemical potential term appears due the configurational entropy of unoccupied sites.

$$\mu_{excess} = K_B T ln(\gamma)$$

Lumping the dilute solution and the excess interaction-induced entropy, we derive that under non-ideal conditions, species activities have to be modified to

$$a_i = \gamma \cdot x\ with\ \gamma = \frac{1}{1-x}$$

Note: γ is approximately 1 under the ideal solution model.

Li-Ion equilibrium potential

Equation of intercalation into a host material M

$$Li^+ + e^- + s \cdot M \rightarrow LiM_s$$

Assuming only negligible change in the enthalpic term of the chemical potential under intercalation (constant temperature, pressure, volume, and internal energy), one can write the total chemical potential at one electrode as:

$$\mu = \mu^\Theta + K_B T \cdot \sum_i s_i \cdot \ln(a_i) + ne\phi = \mu^\Theta + K_B T ln\left(\prod_i a_i^{s_i}\right) + ne\phi$$

Where n, s_i, ϕ, and μ^Θ are respectively the number of electrons exchanged, the stoichiometric constant of species *i* in the reaction, the electrode potential, and the chemical potential at standard conditions.
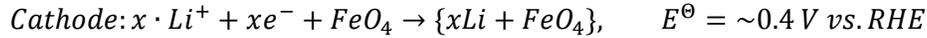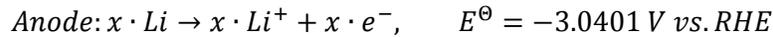
Under the typical intercalation reaction listed above, we can write

$$\phi = \frac{\mu^\Theta}{e} + \frac{K_B T}{e} ln\left(\frac{a_{Li^+} \cdot a_e \cdot a_M^s}{a_{LiM_s}}\right) = \phi^\Theta + \frac{K_B T}{e} ln\left(\frac{a_{Li^+} \cdot a_e \cdot a_M^s}{a_{LiM_s}}\right)$$

Note: In the absence of quantum effects, a_e is set to 1.

<u>Example of LiFePO4</u>

In the case of Li-Ion batteries where monovalent lithium cations are shuttled, $z = 1$

$$Anode: x \cdot Li \rightarrow x \cdot Li^+ + x \cdot e^-, \qquad E^{\Theta} = -3.0401\ V\ vs.\ RHE$$

$$Cathode: x \cdot Li^+ + xe^- + FeO_4 \rightarrow \{xLi + FeO_4\}, \qquad E^{\Theta} = \sim 0.4\ V\ vs.\ RHE$$

$$V_{cell} = \phi_c - \phi_c = \left(0.45 + \frac{KT}{xe} \ln\left(\frac{a_{Li^+}^x \cdot a_{FeO_4}}{a_{Li}^x \cdot a_{FeO_4}} \right) - \left(-3.0401 + \frac{KT}{xe} \ln\left(\frac{a_{Li^+}^+}{a_{Li}^x} \right) \right) \right)$$

Simplification assumptions: standard conditions at the anode and the activity of Li cations in solution and the host FePO4 is 1.

$$V_{cell} = \phi_c - \phi_a = \left(0.45 - \frac{KT}{xe} \ln\left(a_{Li\ in\ FeO_4}^x \right) - \left(-3.0401 + \frac{KT}{xe} \ln(1) \right) \right) = 3.44 - \frac{KT}{e} \ln(a_{Li\ in\ FePO4})$$

Under the ideal solution model,

$$a_{Li} = \frac{x}{1-x} \Rightarrow V_{cell} = 3.44 - 26 \cdot 10^{-3} \ln\left(\frac{x}{1-x} \right)$$
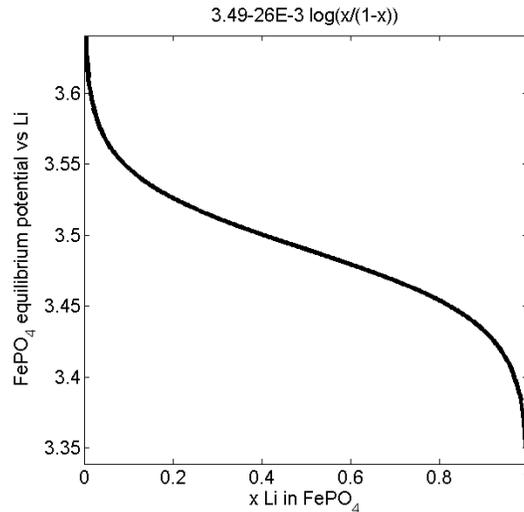
Note: $\frac{KT}{e} \sim 26\ mV\ at\ 25^o C$

Figure 1: Anticipated profile of LiFePO4 electrode potential versus state of discharge using the regular solution model.

Capacitance of Li-Ion batteries under the ideal solution model

As derived previously,

$$\phi_c^{eq} = \phi^{\Theta} - \frac{KT}{e} ln\left(\frac{x}{1-x} \right)$$

Solving for x in tche above expression, we arrive to:

$$x = \frac{1}{2} + \tanh\left[\frac{e\left(\phi^{\Theta} - \phi_c^{eq}\right)}{2K_BT}\right]$$

The amount of charge Q passed in coulomb can therefore be written as function of state of discharge x

$$Q = eC_{max} \cdot x = eC_{max} \cdot \left\{\frac{1}{2} + \tanh\left[\frac{e\left(\phi^{\Theta} - \phi_c^{eq}\right)}{2K_BT}\right]\right\}$$

The faradaic capacitance, assuming that the electrode reactions are fast such that a state of (quasi) is maintained with respect to the applied potential:

$$C_F = -\frac{\partial Q}{\partial V} = \frac{\partial Q}{\partial \phi_c^{eq}} = \frac{e^2 C_{max}}{2K_BT} \operatorname{sech}^2\left(\frac{e\left(\phi^{\Theta} - \phi_c^{eq}\right)}{2K_BT}\right)$$

Under cyclic voltammetry, V(t) = ±r.t, and the quasi-equilibrium assumption

$$Q = eC_{max} \cdot \left\{\frac{1}{2} + \tanh\left[\frac{e(\phi^{\Theta} - r \cdot t)}{2K_BT}\right]\right\} \Rightarrow I(t) = \frac{\partial Q}{\partial t} = \frac{e^2 C_{max}}{2K_BT} r \operatorname{sech}^2\left(\frac{e(\phi^{\Theta} - r \cdot t)}{2K_BT}\right)$$

$$I(t) = \frac{e^2 C_{max}}{2K_BT} r \operatorname{sech}^2\left(\frac{e\left(\phi^{\Theta} - V\right)}{2K_BT}\right)$$

Let's plot this current at room temperature and setting constant parameters to 1 for visualization purposes

$$I(t) = \operatorname{sech}^2(19 \cdot (3.44 - V))$$
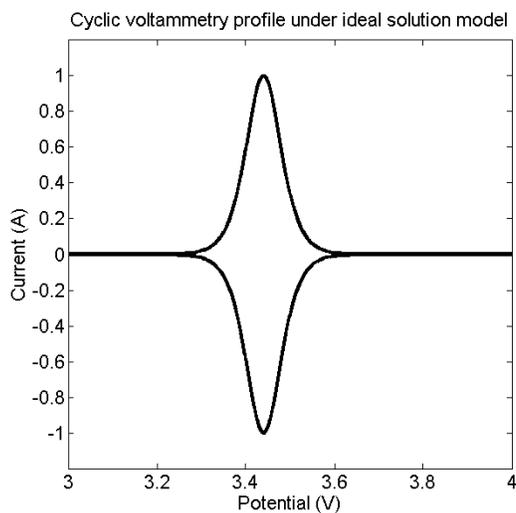

Figure 2: Predicted cyclic voltammetry profile of Li-Ion battery electrodes under the ideal solution model.

Published experimental results: Figures taken from Matsui et al. J. Power Sources 2010, 195, 6879–6883

Figure 3: (left) Open-circuit voltage curves of LiFePO$_4$ particles: open and solid circles denote the measured values during the discharging and charging process, respectively. (right): Cyclic voltammograms under various sweeping rates from 0.01mVs−1 to 1.0 mVs−1 for LiFePO$_4$ particles. Caption taken from paper.

From Figure 3 (right) cyclic voltammogram, we can determine (from the mid-peak potential) that the reversible cell potential using LiFePO$_4$ as cathode is ~3.45 V vs. lithium. Comparing the experimental voltammogram in Figure 3 (right) to the predicted voltammogram from the ideal solution model, one can observe that experimentally a shift is observed between the forward wave compared to the backward wave. This is a consequence of transient non-equilibrium processes (transport for example) which are ignore in the model. The figure on the left shows the open circuit voltage of a Li∥LiFePO$_4$ cell as a function of state of depth of discharge (bottom horizontal axis, open circle symbols). The initial drop, slow decay, and final drop features of the OCV correspond somewhat to the general profile predicted under the ideal solution model shown in Figure 1. However, it is obvious that while the ideal solution model predicts in Figure 1 a continuous decay in the OCV as a function of depth of discharge (DOD), experimental results shown in Figure 3 (left) clearly present a plateau region. Therefore, a different model for the intercalation process is desirable.

Regular solution model

We recall that derivation of the entropic term of the chemical potential shown above relied on the assumption of *ideal* lattice gas. In reality, intercalating ions interact due to quantum effects, site exclusion, and crowding (especially at high concentrations of inserted cations where the "dilute solution" assumptions no longer reasonably holds). These interactions result in additional energy added to the ideal dilute solution chemical potential. These additional terms can be expressed as follows:

$$g(x) = K_B T[x \ln x + (1-x)\ln(1-x)] + h_o x(1-x) + \mu_0 \cdot x$$

$$h_o x(1-x): pair\ interaction\ energy\ between\ particles\ and\ holes$$

Note: h$_0$ is positive when attraction exists between intercalated particles (to increase the system energy) and negative when repulsion exists between particles (to decrease the systems free energy). μ$_0$ reflects the system internal energy.

Under this model then,

$$\mu = K_B T ln\left(\frac{x}{1-x}\right) + h_0(1-2x) + \mu_0$$

$$\phi_{eq} = \phi^\Theta - \frac{K_B T}{e} ln\left(\frac{x}{1-x}\right) - \frac{h_0}{e}(1-2x)$$

On the one hand, at high temperatures, the configuration entropy term is large enough to dominate the free energy surface resulting in the ideal solution model being a good approximation to the intercalation process.

At reasonably low temperatures (say room temperature), non-ideal interactions are significant and result in interesting features in the free energy profile as a function of state of discharge x.
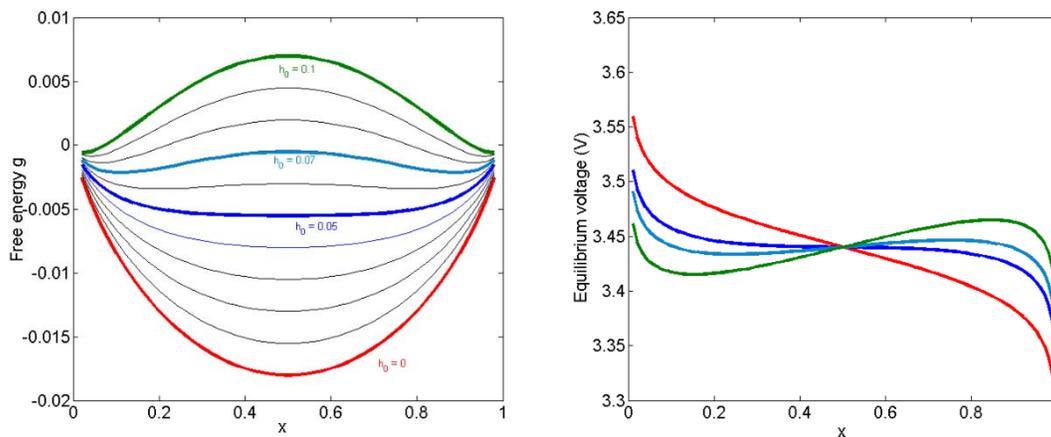

Figure 4: (left) Free energy as a function of state of discharge x and interaction enthalpy factor at room temperature with $\mu_0 = 0$. (right) Cell equilibrium potential under regular solution model. A color correspondence is maintained between the left and right graphs.

Four cases of the free energy surface are observed in Figure 4.

- At h_0 equal zero (red curves) corresponding to the absence of pair interactions, one minimum is observed on the free energy versus state of charge signifying that one phase at x=1/2 is stable. This is the case of the ideal solution model and a similar voltage profile to the one above is retrieved.
- At h_0 equal 0.05 (dark blue curves), a flat "minimum" region appears on the free energy surface and indicates that most phases (x ~ 0.2 to 0.8) are reasonably stable and can coexist during discharge. This is a critical value of the pair interaction enthalpy. Because most phases (x) are stable, a flat plateau is observed for the voltage profile.
- At h_0 equal 0.07 (navy blue curves), two minima appear and indicates 2 stable phases. The voltage profile has an inflection point. In reality, a mixture of the two stable phases will be observed resulting in the system following a common tangent joining the two energy minima. This in turn will result in plateau profile for the electrode potential away from the filling extrema.
- At even greater values of h0 (green curves), attraction between intercalated particles is so large that no stable homogeneous phase can exist in the system. The phase is highly susceptible to perturbations. The voltage profile first decays at the low ends of filling. It then rises as high attraction between particles causes inhomogeneous filling leaving empty areas in the host materials

favorable to filling. Finally at very high average filling, the cell voltage decays due to complete occupancy of all available sites.

Faradaic Capacitance in Li-Ion batteries under regular solution model

$$Q = eC_{max} \cdot x \text{ and } I(t) = \frac{\partial Q}{\partial t} = r \cdot \frac{\partial Q}{\partial V}$$

For the purpose of visualization, let's set $eC_{max} = 1$ and $r = 1$ and solve numerically
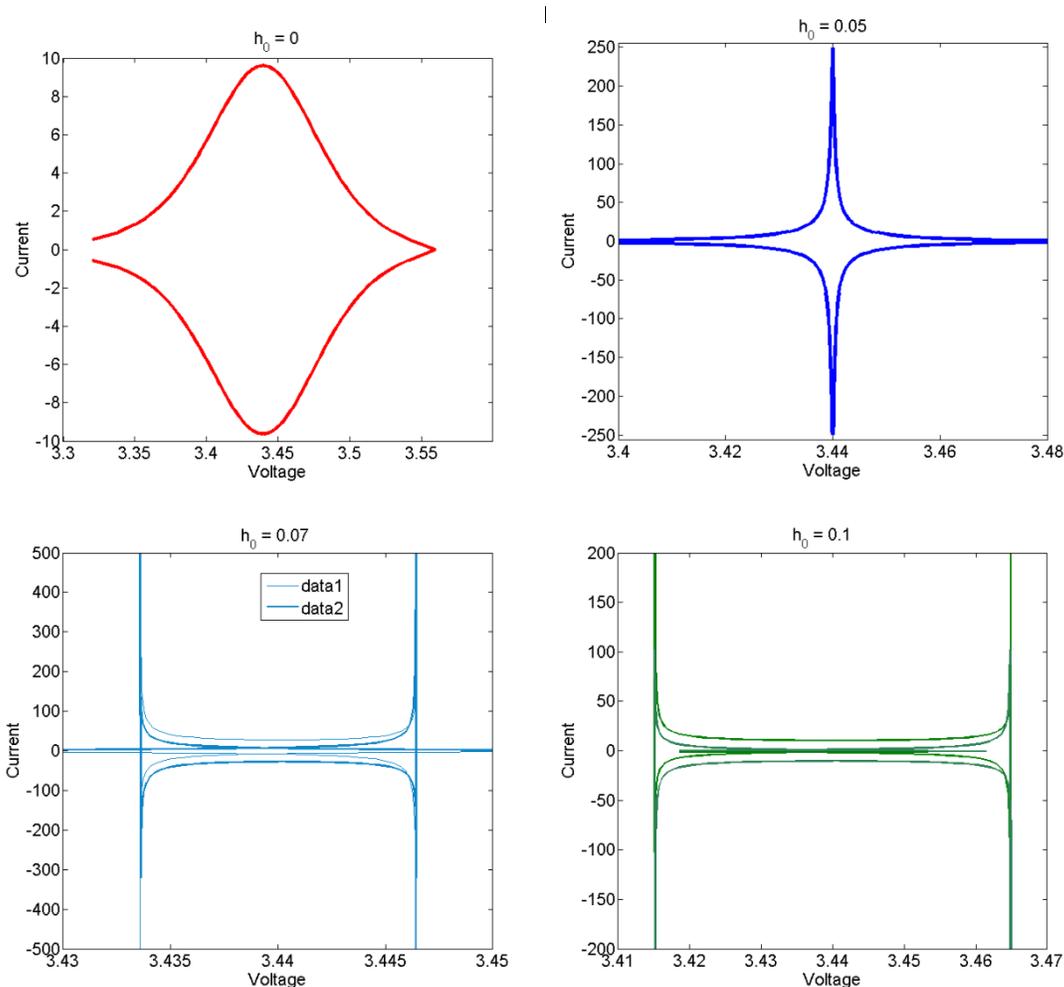

Figure 5: Current vs. potential under sweep voltammetry using the regular solution model for key values of the interaction enthalpy. A color correspondence is maintained between the capacitance curves and the free energy and potential curves in Figure 4.

Once again, four cases of the free energy surface are observed in Figure 5 corresponding to each situations on the free energy surfaces.

- At h_0 equal zero, the capacitance curve for the ideal solution model is recovered by the regular solution model.
- A h_0 equal 0.05, a most of the current is delivered catastrophically close to the equilibrium potential due to the stability of most phases (in terms of x).

- For the two phase solution at h_0 equal 0.07, within the miscibility gap, the capacitance behave much like an electrostatic capacitor.

Further information and nomenclatures for phase separating
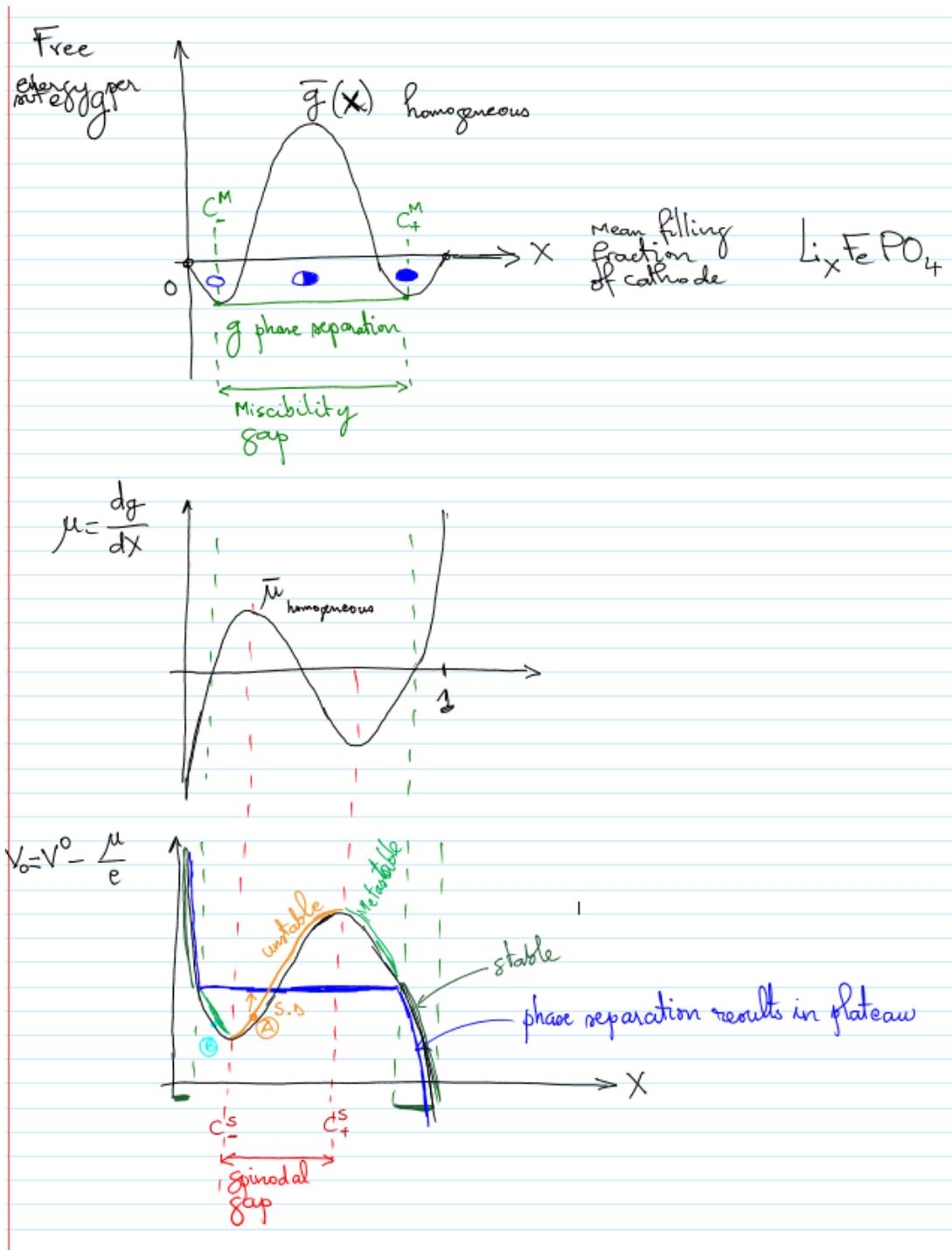
10.626 Electrochemical Energy Systems
Spring 2014